THE 1995 AVIRIS GEOLOGY GROUP SHOOT

Fred A. Kruse
Analytical Imaging and Geophysics LLC
Louisville, Colorado 80027 USA
and
Jonathan F. Huntington
CSIRO, Division of Exploration and Mining
North Ryde, NSW 8112, Australia

1. INTRODUCTION

An Airborne Visible/Infrared Imaging Spectrometer (AVIRIS) geology "Group Shoot" was conducted during summer 1995 by Analytical Imaging and Geophysics (AIG) in cooperation with the CSIRO Division of Exploration and Mining, NASA Ames Research Center, and the Jet Propulsion Laboratory/California Institute of Technology (JPL). The purpose of this effort was to give mining companies and other interested commercial entities a chance to acquire high quality imaging spectrometer data for selected sites of specific interest.

AIG/CSIRO determined company interest, compiled targets and signed an MOU and Space Act Agreement with NASA prior to the mission. Funds were collected from company sponsors and forwarded to NASA Ames Research Center in accordance with these agreements. The sites were flown in late July 1995 under near-optimum conditions. High quality AVIRIS data were collected during this mission for sites in Arizona, Nevada, California, Utah, Wyoming, and Colorado, USA. A typical site consisted of two-to-four approximately 10 x 12 km AVIRIS scenes. While the original mission concept was to have all of the sites flown on one day, the geographic spread of the sponsors' sites and weather conditions at the sites required both NASA and AIG to be flexible in scheduling acquisitions. Table 1 gives a list of sites acquired. Figure 1 shows the approximate locations of the sites, the number of scenes acquired, and the date of data acquisition.

Table 1. Sites Flown During 1995 AIG/CSIRO AVIRIS Group Shoot

SITE	LAT 1/LON 1	LAT 2/LON 2
1) Cheyenne WY (Nunn, CO)	N40d 48m 15s/W104d 27m	N40d 48m 15s/W104d 52m 30s
2) Lander, WY	N42d 35m 16s/W108d 39m 36s	Center Point for 2 scenes, Fly grid az of 90 or 270 degrees
3) Tintic, UT	N39d 48m 27.61s/W112d 06m 35.94s	N39d 59m 16.21s/W112d 06m 45.82s
4) S. Oqhirrh Mtns, UT	N40d 14m 37.77s/W112d 8m 52.35s	N40d 23m 25.85s/W112d 17m 4.29s
5) Mule Ear 1, UT	N37d 2m 30s/W109d 50m	N37d 15m/W109d 40m
Mule Ear 2, UT	N37d 13m/W109d 44m	N37d 3m/W109d 46m
6) Railroad Valley, NV	N38d 37' 2.2/W115d 37' 17.9W	Center Point for 4 scenes, Fly grid AZ of 115d or 295degrees
7) Goldfield, NV	N37d 50m/W117d 13m	N37d 24m/W117d 13m
8) Oatman, AZ	N35d 07m 30s/W114d 25m	N34d 58m 30s/W114d 25m
9) Virginia City, NV #1	N39d 10m/W119d 43m	N39d 26m/W119d 34m
Virginia City, NV #2	N39d 25m/W119d 45m	N39d 15m/W119d 35m

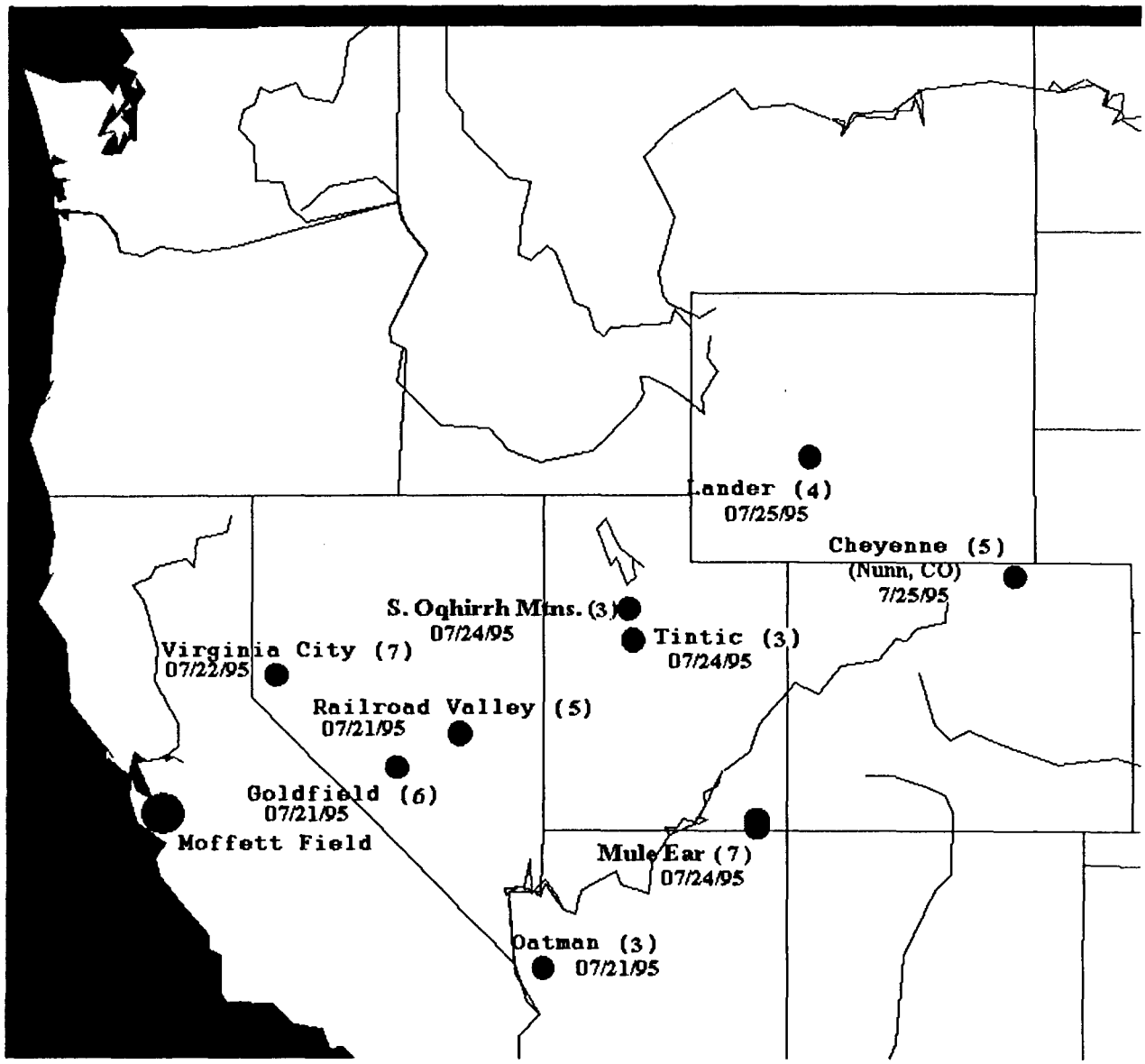

Figure 1. AIG/CSIRO Group Shoot Approximate Target Locations, Number of Scenes Acquired, and Data Acquisition Dates.

2. INSTRUMENT INFORMATION

The Airborne Visible/Infrared Imaging Spectrometer (AVIRIS) is an imaging spectrometer that simultaneously acquires 224 spectral images at 20 meter spatial resolution and 10 nanometer spectral resolution. Each "scene" covers an approximately 10 x 12 kilometer area. Imaging spectrometers collect images, however, in addition, a complete spectrum can also be extracted from each picture element (pixel) of the image, thus allowing detailed mapping based on the spectroscopic characteristics of minerals (Goetz et al., 1985, Boardman et al., 1995).

Despite major revisions to the instrument prior to the 1995 flight season, AVIRIS operated without problems during the Group Shoot flights. Some minor irregularities were

observed with the data, however, the order of magnitude of these is near the noise level in the data (R.O. Green, Personal Communication). Problems encountered with the data included 1) dropped bits in individual pixels resulting in anomalous spectra, 2) multiplexer lag in the instrument resulting in spatial shifting between bands (bands 13 and 35 were discarded because of a 1 pixel or greater shift). According to Rob Green at JPL, "the multiplexer lag artifact is similar to the detector-readout-delay that has been in all AVIRIS data before 1995. The artifact expresses itself very close to the level of the AVIRIS noise." What this means, is that the size of the instantaneous field of view (IFOV) of AVIRIS varies slightly as a function of the intensity of the signal. According to Green, the AVIRIS calibration without any correction is still at the 96% level. Based on preview processing by AIG, the AVIRIS data were judged to be satisfactory for the purposes of flight sponsors. In general, the data appeared to be of high quality in both the spatial and spectral domains.

3. THE GOLDFIELD/CUPRITE GROUP SITE

The Goldfield/Cuprite area, Nevada, was chosen by AIG as the shared group site for the 1995 AVIRIS Group Shoot because considerable previous remote sensing information exists for the area, and AIG principals have analyzed previous AVIRIS acquisitions for these sites and conducted field verification studies. This site acted as the "control" for the 1995 AVIRIS data acquisition and the processing performed was useful as an example for the other sites. Four AVIRIS scenes were analyzed. Table 3 outlines AIG's "standardized" procedure for analyzing AVIRIS data for a typical site.

Table 3. AIG "Standardized" AVIRIS Processing Methodology

1. Download Quicklook Data
2. Review Spatial Coverage
3. Preliminary Assessment of Spatial Data Quality
4. Define Areas for Further Processing
5. Order AVIRIS Radiance Data for Selected Scenes
6. Download Radiance Data from Tape
7. Data Quality Assessment
   - Spatial Browsing
   - Spectral Browsing
   - SNR Calculations
8. Calibration to Apparent Reflectance
   - ATREM
   - Empirical Line Calibration if ground information available
   - "Eff" correction if no ground information available
   - Spectral Browsing
9. Report Data Problems to JPL
10. MNF Transform
11. Pixel Purity Index
12. n-Dimensional Visualization (Endmember Definition)
13. Spectral Angle Mapper (SAM)
14. Spectral Unmixing and/or Match Filtering
15. Annotation, Output, and Report

3.1 Download Quicklook Data

JPL processing to AVIRIS Quicklooks for some sites was completed within two weeks, with all of the quicklook processing completed by mid-August 1995. Quicklook data were obtained via anonymous FTP from JPL on-line at: "ophelia.jpl.nasa.gov" in the directory "/pub/95qlook. AIG downloaded the quicklooks for all of the sites, reviewed the spatial coverage and produced hardcopy output, which was provided to the sponsors. All of the requested sites were covered per the flight specifications. Standard processed, full AVIRIS scenes for each site were ordered from JPL following the preview by AIG. Initial radiance data arrived the last week in September and the first week in October. AIG copied the data tapes and provided datasets to each of the sponsors for evaluation. The Goldfield/Cuprite data were calibrated to reflectance by AIG and processed to mineral maps to assess the data quality. This processing is discussed below.

3.2 Read Data From Tape

The Goldfield/Cuprite AVIRIS data and wavelength file were read from tape on a SUN SPARC system in Band-Interleaved-by-Line (BIL) format.

3.3 Preview Data and Assess Quality

Calibrated radiance data were both spatially and spectrally previewed. The spatial coverage of the two sites was good and the spatial fidelity of the data was excellent. Spatial browsing of different bands indicated that bands 13 and 35 were spatially offset from the rest of the bands (by one pixel horizontally. Another apparent anomaly was that some pixels exhibited what appeared to be dropped bits in one or more spectral bands. This was only for about 10-30 pixels per 614 x 1024 scene, or well less than 1% of the data. These were not used in subsequent processing.

3.4 ATREM Calibration

The Goldfield/Cuprite AVIRIS data were initially calibrated to apparent reflectance using the "ATREM" software available from the Center for the Study of Earth from Space (CSES) at the University of Colorado, Boulder. This software can be obtained via anonymous FTP from "cses.colorado.edu" in the directory "pub/atrem. Get the readme file for download instructions.

ATREM is an atmospheric model-based calibration routine, and requires input of data parameters such as the acquisition date and time, the latitude and longitude of the scene, and the average elevation, along with atmospheric model parameters (CSES, 1992). AIG used the ATREM version 1.31, which had to be updated to work with the 1995 data. An updated version should be available for most UNIX platforms from CSES. The output of the ATREM procedure is apparent reflectance calibrated data and a water vapor image for each scene. Typically, the water vapor image mimics topographic expression. Higher water vapor concentrations occur in the valleys, and lower water vapor concentrations over the higher elevations. In the Goldfield/Cuprite case, however, it appears as if there may have been some modulation by clouds. No clouds were visible in the images, however, and the ATREM apparent reflectance data appear to have adequately removed water vapor contributions from the spectra.

3.5 Evaluate Apparent Reflectance Data

Spectral browsing through both the apparent reflectance calibrated Goldfield and Cuprite data sets was used to get an idea of the success of the calibration as well as to identify specific minerals. This procedure indicated that the spectral quality of the data was excellent and the apparent reflectance calibration adequate. Band bands at 0.5001 μm (band 13) and 0.6824 μm (band 35), the overlap regions between spectrometers in bands 32-34 (~0.67 μm) and in bands 97-98 (~1.26 μm), as well as the spectral regions between approximately 1.3 - 1.4 μm and 1.84 and 1.96 μm corresponding to the major atmospheric water bands were masked out during subsequent processing. Individual spectra could be recognized in the apparent reflectance calibrated data that contained absorption features attributable to kaolinite, alunite, buddingtonite, muscovite, and calcite (Figure 2).

3.6 MNF Transformation

The next step of the processing was to perform a "Minimum Noise Fraction" (MNF) Transform to reduce the number of spectral dimensions to be analyzed. The MNF transformation is used to determine the inherent dimensionality of the data, to segregated noise in the data, and to reduce the computational requirements for subsequent processing (Green et al., 1988; Boardman and Kruse, 1994). The process is essentially two cascaded Principal Components transformations. The first transformation, based on an estimated noise covariance matrix decorrelates and rescales the noise in the data. This results in data in which the noise has unit variance and no band-to band correlations. The second step is a standard PC transformation of the noise-whitened data. The inherent dimensionality of the data is determined by examination of the eigenvalues and associated eigenimages. The data space is divided into two parts: one associated with large eigenvalues and coherent eigenimages, and a second with near-unity eigenvalues and noise-dominated images. By using only the coherent portions in subsequent processing, the noise is separated from the data, thus improving spectral processing results. Similar results are obtained when the MNF transformation is run on either the Goldfield or the Cuprite AVIRIS data. The eigenvalue plots fall sharply for the first 10 eigenvalues and flatten out. Examination of the eigenimages shows that while the first 10 images contain most of the information, images 11 through 20 still contain coherent spatial detail. The higher numbered MNF bands contain progressively lower signal-to-noise. Vertical bands, probably caused by multiple scattering in the AVIRIS optical path were observed in the visible-region MNF bands 7 - 11. This problem was reported to JPL.

3.7 Pixel Purity Index (PPI)

Based on the above MNF results, the lower order MNF bands were discarded and the first 20 MNF bands were selected for further processing. These were used in the "Pixel Purity Index" (PPI), processing designed to locate the most spectrally extreme (unique or different or "pure") pixels (Boardman et al., 1995). The most spectrally pure pixels typically correspond to mixing endmembers. The PPI is computed by repeatedly projecting n-dimensional scatterplots onto a random unit vector. The extreme pixels in each projection are recorded and the total number of times each pixel is marked as extreme is noted. A PPI image is created in which the digital number of each pixel corresponds to the number of times that pixel was recorded as extreme. A histogram of these images shows the distribution of "hits" by the PPI. A threshold was interactively selected using the histogram and used to select only the purest pixels in order to

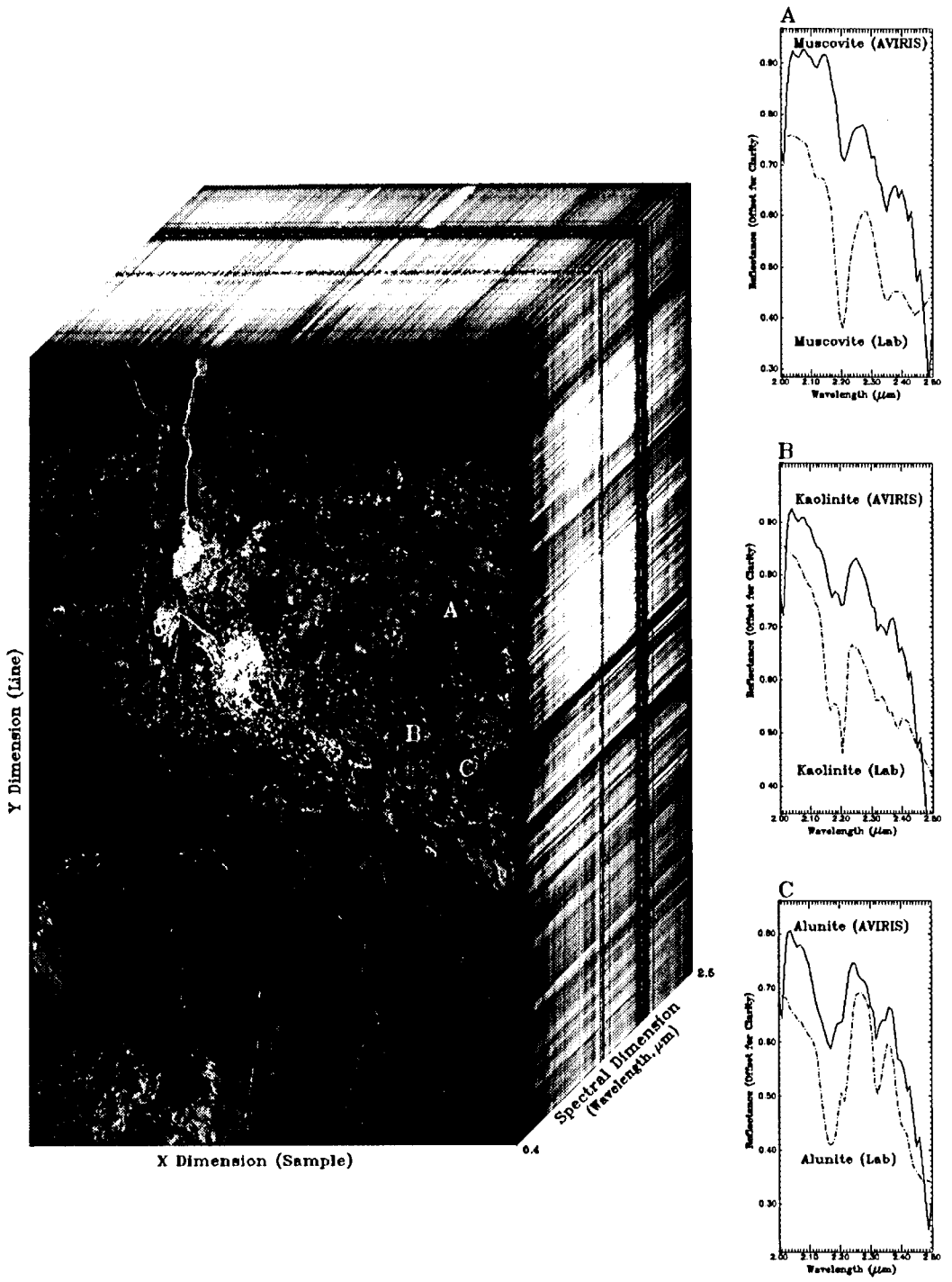

Figure 2. 3-D perspective cube of band 30 (0.67 μm) for the Goldfield 1995 AVIRIS site. Representative AVIRIS spectra are compared to Library Spectra on the right.

keep the number of pixels to be analyzed to a minimum. These pixels were used as input to an interactive visualization procedure for separation of specific endmembers.

3.8 n-Dimensional Visualization

Spectra can be thought of as points in an n-dimensional scatterplot, where n is the number of bands (Boardman, 1993; Boardman et al., 1995). The coordinates of the points in n-space consist of "n" values that are simply the spectral reflectance values in each band for a given pixel. The distribution of these points in n-space can be used to estimate the number of spectral endmembers and their pure spectral signatures. This geometric model provides an intuitive means to understand the spectral characteristics of materials. In two dimensions, if only two endmembers mix, then the mixed pixels will fall in a line in the histogram. The pure endmembers will fall at the two ends of the mixing line. If three endmembers mix, then the mixed pixels will fall inside a triangle, four inside a tetrahedron, and so on. Mixtures of endmembers "fill in" between the endmembers. All mixed spectra are "interior" to the pure endmembers, inside the simplex formed by the endmember vertices, because all the abundances are positive and sum to unity. This "convex set" of mixed pixels can be used to determine how many endmembers are present and to estimate their spectra.

The Goldfield/Cuprite AVIRIS dataset were analyzed using these geometric techniques. The thresholded pixels from the MNF images above were loaded into an n-dimensional scatterplot and rotated in real time on the computer screen until "points" or extremities on the scatterplot were exposed. These projections were "painted" using Region-of-Interest (ROI) definition procedures and then rotated again in 3 or more dimensions (3 or more bands) to determine if their signatures were unique in the AVIRIS MNF data. Once a set of unique pixels were defined, then each separate projection on the scatterplot (corresponding to a pure endmember) was exported to a ROI in the image. Mean spectra were then extracted for each ROI to act as endmembers for spectral unmixing. Using the IR data only from 2.0 to 2.4 μm, 9 endmembers were defined for the Goldfield/Cuprite AVIRIS data. These include the minerals calcite, buddingtonite, kaolinite, muscovite, alunite, and zeolite-group minerals. Another mineral, with an "unknown 2.2 μm absorption feature" was also located. Based on the spatial distribution of spectra matching this endmember and known information about the sites, this endmember was identified as representing opaline silica. Unfortunately, similar spectra also occur on alluvial fans away from the altered areas, probably because of weathering and/or spectral mixing. Finally, both "light" and "dark", relatively aspectral endmembers were defined. These endmembers or a subset of these endmembers were used for subsequent classification and other processing.

3.9 Spectral Angle Mapper (SAM) Classification

The Spectral Angle Mapper (SAM) is an automated method for comparing image spectra to individual spectra (Boardman, Unpublished data; Kruse et al., 1993). The algorithm determines the similarity between two spectra by calculating the "spectral angle" between them, treating them as vectors in a space with dimensionality equal to the number of bands. Because this method uses only the vector "direction" of the spectra and not their vector "length", the method is insensitive to illumination. The result of the SAM classification (not shown) is an image showing the best SAM match at each pixel. Additionally, rule images are calculated that

show the actual angular distance (in radians) between each spectrum in the image and each reference or endmember spectrum. Darker pixels in the rule images represent smaller spectral angles and thus spectra that are more similar to the endmember spectra. For the purposes of display, the dark pixels are inverted, so that the best matches appear bright. These images present a good first cut of the mineralogy at the sites.

3.10 Spectral Unmixing

While the SAM algorithm does provide a means of identifying and spatially mapping minerals, it only picks the best match to a spectrum. Natural surfaces are rarely composed of a single uniform material, thus it is necessary to use mixture modeling to determine what materials cause a particular spectral "signature" in imaging spectrometer data. Spectral mixing is a consequence of the mixing of materials having different spectral properties within a single image pixel. If the scale of the mixing is large (macroscopic), then the mixing occurs in a linear fashion. A simple additive linear model can be used to estimate the abundances of the materials measured by the imaging spectrometer. Each mixed spectrum is a linear combination of the "pure" spectra, each weighted by their fractional abundance within the pixel, a simple averaging (Boardman, 1991).

In order to determine the abundances, we must first determine what materials are mixing together to give us the spectral signature measured by the instrument. Selection of "endmembers" is the most difficult part of linear spectral unmixing. The ideal spectral library used for unmixing consists of endmembers that when linearly combined can form all other observed spectra. This can be presented as a simple mathematical model in which the observed spectrum (a vector) is the result of a multiplication of the mixing library of pure endmember spectra (a matrix) by the endmember abundances (a vector). An inverse of the original spectral library matrix is formed by multiplying together the transposes of the orthogonal matrices and the reciprocal values of the diagonal matrix (Boardman, 1989). A simple vector-matrix multiplication between the inverse library matrix and an observed mixed spectrum gives an estimate of the abundance of the library endmembers for the unknown spectrum.

Linear Spectral Unmixing was used as the final step in producing mineral maps for the Goldfield/Cuprite AVIRIS data. The endmember library defined using the n-dimensional visualization procedure was used in the unmixing process and abundance estimates were made for each mineral. These results can be presented in two ways. First, a set of gray-scale images stretched from 0 to 50% (black to white) provides a means of estimating relative mineral abundances. These results are shown in Figure 3. Secondly, color composite images can be used to highlight specific minerals and mineral assemblages. Pure colors in these images represent areas where the mineralogy is relatively pure. Mixed colors indicate spectral mixing, with the resultant colors indicating how much mixing is taking place and the relative contributions of each endmember. For example, in a color composite for Goldfield (not shown), the minerals Kaolinite, Alunite, and Muscovite when assigned to Red, Green, and Blue in the color output result in distinctive image colors. Areas that are pure red in such an image correspond to areas where kaolinite is the spectrally dominant (~most abundant) mineral. Areas that are green are dominated by Alunite. Areas that are blue contain primarily muscovite. The yellow pixels are an example of mixed pixels, where the contribution of red from kaolinite and of green from alunite results in the mixed yellow color.

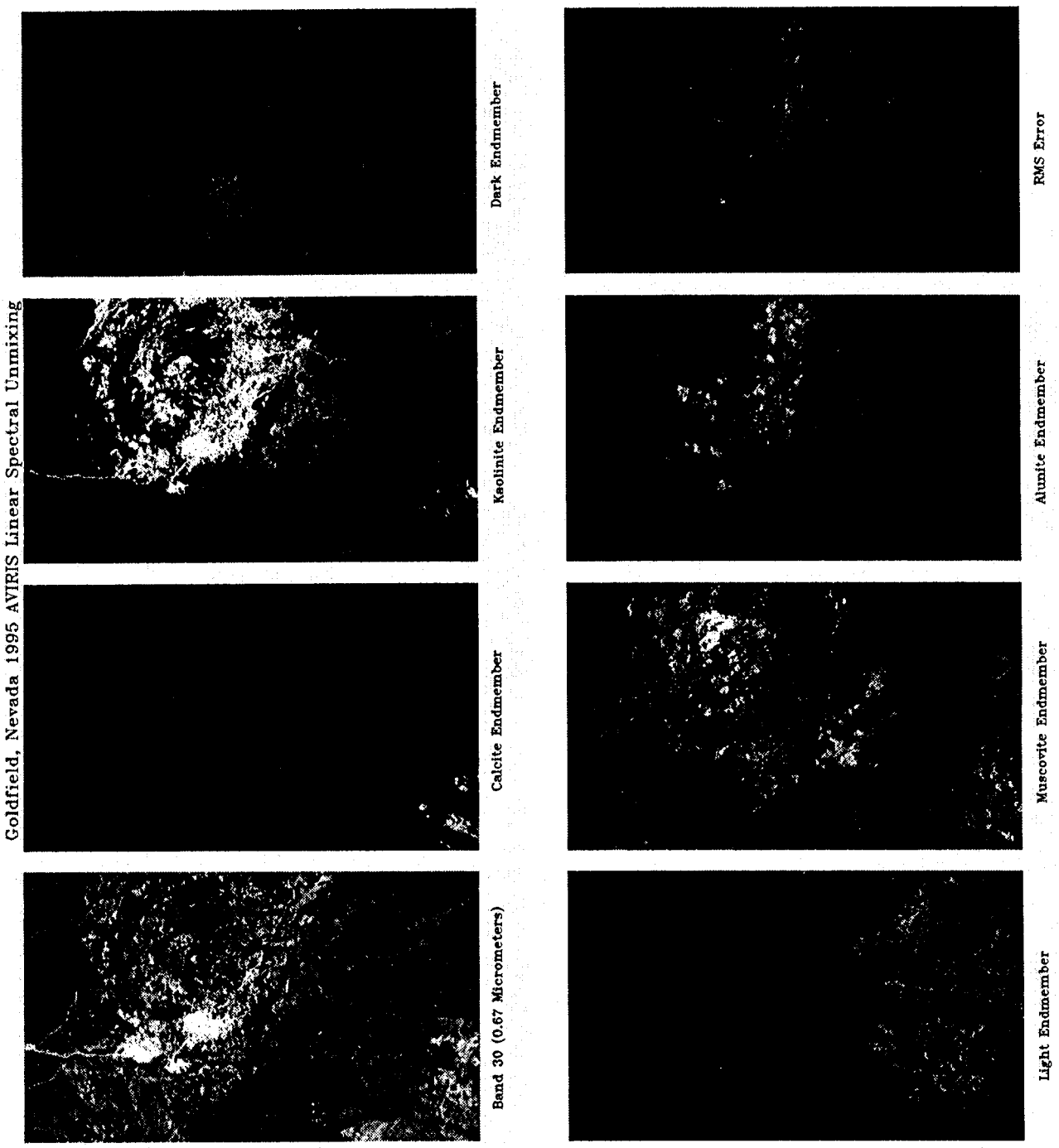

Figure 3. 1995 Goldfield AVIRIS Unmixing Results. Bright pixels represent higher abundances stretched from 0 - 50% (black to white).

4. CONCLUSIONS

This paper summarizes the organization, data collection, and group-site processing of the 1995 AVIRIS Group Shoot organized by Analytical Imaging and Geophysics. Data were successfully acquired for all sponsors' sites, and data delivery and processing have been completed. AIG has processed the shared group site data for Goldfield/Cuprite and used these well-known sites to define a "standardized" analysis strategy. This methodology was successfully used to produce detailed mineral maps of the Group Site and other sponsors' sites.

This Group Shoot effort has demonstrated that a cooperative industry/NASA effort can provide an efficient means for organizations to share some of the costs and apparent risks of using a new technology while getting data specific to their needs. Based on the results of this Group Shoot, AIG plans to organize and conduct a similar mission during the summer of 1996.

5. REFERENCES

Boardman, J. W., 1989, Inversion of imaging spectrometry data using singular value decomposition,: in Proceedings: IGARSS '89, 12th Canadian Symposium on Remote Sensing, V. 4, p. 2069 - 2072.

Boardman, J. W., 1991, Sedimentary facies analysis using imaging spectrometry: A Geophysical Inverse Problem: Unpublished Ph. D. Thesis, University of Colorado, Boulder, 212 p.

Boardman, J. W., 1993, Automated spectral unmixing of AVIRIS data using convex geometry concepts: in Summaries, Fourth JPL Airborne Geoscience Workshop, JPL Publication 93-26, v. 1, p. 11-14

Boardman, J. W., and Kruse, F. A., 1994, Automated spectral analysis: A geologic example using AVIRIS data, north Grapevine Mountains, Nevada: in Proceedings, Tenth Thematic conference on Geologic Remote Sensing, Environmental Research Institute of Michigan, Ann Arbor, MI, p. I-407 - I-418.

Boardman, J. W., Kruse, F. A., and Green, R. O., 1995, Mapping target signatures via partial unmixing of AVIRIS data: in Summaries, Fifth JPL Airborne Earth Science Workshop, JPL Publication 95-1, v. 1., p. 23 - 26.

CSES, 1992, Atmosphere REMoval Program (ATREM) User's Guide, Version 1.1, Center for the Study of Earth from Space, Boulder, Colorado, 24 p.

Goetz, A. F. H., Vane, G., Solomon, J. E., and Rock , B. N., 1985, Imaging spectrometry for earth remote sensing: Science, v. 228, p. 1147 - 1153.

Green, A. A., Berman, M., Switzer, B., and Craig, M. D., 1988, A transformation for ordering multispectral data in terms of image quality with implications for noise removal: IEEE Transactions on Geoscience and Remote Sensing, v. 26, no. 1, p. 65 - 74.

Kruse, F. A., Lefkoff, A. B., Boardman, J. B., Heidebrecht, K. B., Shapiro, A. T., Barloon, P. J., and Goetz, A. F. H., 1993, The Spectral Image Processing System (SIPS) - Interactive Visualization and Analysis of Imaging Spectrometer Data: Remote Sensing of Environment, Special issue on AVIRIS, May-June 1993, v. 44, p. 145 - 163.